Proceedings of the International Conference on Heat Transfer and Fluid Flow
Prague, Czech Republic, August 11-12, 2014
Paper No. 192

Computational Modelling of the Surface Roughness Effects on the Thermal-elastohydrodynamic Lubrication Problem

Shian Gao
Department of Engineering, University of Leicester
University Road, Leicester LE1 7RH, UK
sg32@le.ac.uk

Sutthinan Srirattayawong
School of Engineering, University of Phayao
19 Moo 2, Maeka, Muang, Phayao 56000, Thailand
hungaong@yahoo.com

Abstract **-**In this paper, the behaviour of the Thermal-Elastohydrodynamic Lubrication (TEHL) line contact with measured surface roughness for different materials is studied using an advanced Computational Fluid Dynamics (CFD) model, instead of using the classical Reynolds equation. The Ree-Eyring model is used to calculate the viscosity of lubricant, and the surface of cylindrical roller bearing is defined to have a real roughness, while the plate surface is defined as smooth. The characteristics of the TEHL such as the pressure distribution, the film thickness, the velocity of fluid flow, the viscosity and the temperature distribution are investigated under various conditions. The results show clearly the significance of the surface roughness on the lubricant flow, especially at the contact centre region. In addition the fluctuated flow also affects the pressure distribution, the temperature and the lubricant viscosity in a similar pattern to the rough surface profile.

Keywords**:** Thermal effects, Elastohydrodynamic, Surface roughness, CFD, Non-Newtonian.

1. Introduction

It is well known that bearing is very important in machines as it can reduce the friction losses and increase the efficiency of machines. In addition, the lubrication system is also significant to the life of machines. In order to study the lubrication problem, it is necessary to consider many effecting factors, including the roughness of the bearing surface. Many researchers have developed different methods, simple or complex, for solving such problems.

Osborne Reynolds (Reynolds, 1886) presented the differential equation that is used to state the relationship between the motion and viscosity of the lubricant. The Reynolds equation has since been used to describe laminar flows for the Newtonian fluids in the hydrodynamics lubrication problems. Hertz (1881) studied the deformation of solids that are in dry contact and developed the elasticity theory to determine the resultant stresses between two spherical bodies. The Hertz theory for elastic deformation is widely accepted and is considered to be the foundation for solving the Elastohydrodynamic Lubrication (EHL) problems.

Since the EHL line contact problem under steady state conditions was firstly solved by numerical method by Petrusevich (1951). Many numerical techniques were proposed to solve the Reynolds equation that is a nonlinear differential equation that requires special numerical techniques for a solution. Dowson and Higginson (1959) suggested a numerical method (Inverse method) applicable to the EHL line contact problems, mainly suitable for highly loaded cases. Okamura (1983) applied the Newton Raphson method to the solution of the Reynolds equation so as to avoid the problem using iteration methods. Hamrock and Dowson (1976) published their work on how Gauss Seidel relaxation can be applied to the EHL point contact problem. The Gauss Seidel technique is successful when it is used to solve the EHL line contact problem, but this technique still takes a long time to converge in the case of a point contact. Lubrecht, et al. (1987) suggested the use of a multigrid technique, designed to significantly speed up the evaluation of the iterative solver. Since then, many other techniques were proposed for reducing the simulation time, such as adaptive meshing, multigrid-multilevel and muti-integration (Osborn and Sadeghi, 1992; Lee and Hsu, 1994).

The effects of surface roughness on hydrodynamic lubrication problems were usually studied by creating a model with a general roughness pattern, and most roughness models were included in the film thickness equation (Ai and Cheng, 1994). The effects of surface roughness on the EHL problem under steady state condition were studied by Venner and Napel (1992), who determined the roughness profile by measuring the actual surface of the material. They found that the surface texture significantly influences the pressure profile and the film thickness.

The modified Reynolds equation (Dowson, 1962; Dowson and Higginson, 1966) is widely used and accepted as the classical method to describe the EHL problem for a long time, but this method still has some limitations such as in the cavitation case. Furthermore, in this model the pressure is assumed to be constant across the film thickness. The pressure gradient is very important in the thermal case, as a high pressure gradient can be the cause of generated heat. In recent years, advances in CFD technique have progressed significantly, and commercial software capable of modelling fluid flows is readily available (Almqvist and Larsson, 2002, 2008). Also, improvements in computer processors mean data can be evaluated quickly. So using CFD simulation programs allows researchers to study and analyse the characteristics of fluid flow without creating the real physical model (Bruyere et al., 2011; Hartinger et al., 2008). Therefore, the CFD approach is chosen in this study to investigate the effects of the real surface roughness on the TEHL problem.

2. Computational Models

2. 1. The Governing Equations

The characteristics of fluid flow can be described by the conservation form of the fluid flow which includes the continuity equation, momentum equation and the energy equation as shown below:

$$\frac{\partial \rho}{\partial t} + \nabla \cdot (\rho \mathbf{u}) = 0 \tag{1}$$

$$\frac{\partial (\rho \mathbf{u})}{\partial t} + \nabla \cdot (\rho \mathbf{u}\mathbf{u}) = -\nabla p + \nabla \cdot \tau \tag{2}$$

where

$$\tau = -\eta\left(\nabla \mathbf{u} + (\nabla \mathbf{u})^T\right) + \frac{2}{3}\eta \mathbf{I} \nabla \cdot \mathbf{u} \tag{3}$$

$$\frac{\partial (\rho T)}{\partial t} + \nabla \cdot (\rho \mathbf{u} T) = \nabla \cdot (k \nabla T) + S_T \tag{4}$$

where

$$S_T = Q_{shear} + Q_{compress} \tag{5}$$

$$Q_{shear} = \eta\left(\nabla \mathbf{u} : \nabla \mathbf{u} + \nabla \mathbf{u} : (\nabla \mathbf{u})^T - \frac{2}{3}(\nabla \cdot \mathbf{u})^2\right) \tag{6}$$

$$Q_{compress} = -\frac{T}{\rho}\left(\frac{\partial \rho}{\partial T}\right)(\mathbf{u} \cdot \nabla p) \tag{7}$$

2. 2. The Film Thickness Equation

The lubricant film between the cylindrical roller bearing and the plate is assumed to be a full film contact. The minimum gap, the cylinder shape, the rough profile and the elastic deformation terms are expressed to be a film thickness formula which is given by

$$h_i = h_o + \frac{x^2}{2R} + R(i) - \frac{4}{\pi E'} \int_{x_{in}}^{x_{out}} p(\xi) \ln\left|\frac{x-\xi}{x_o}\right| d\xi \tag{8}$$

where $R(i)$ is the y-coordinate of the roughness profile.

The geometry and the generated mesh are depicted as shown in Figure 1. The surface of the cylindrical roller bearing is a rough surface, while the plate surface is smooth. In order to predict the real physics of the thin film lubrication, it is necessary to minimize the used assumptions. Therefore the real profile of the surface roughness as shown in Figure 2 is applied to the calculation in the equation (8).

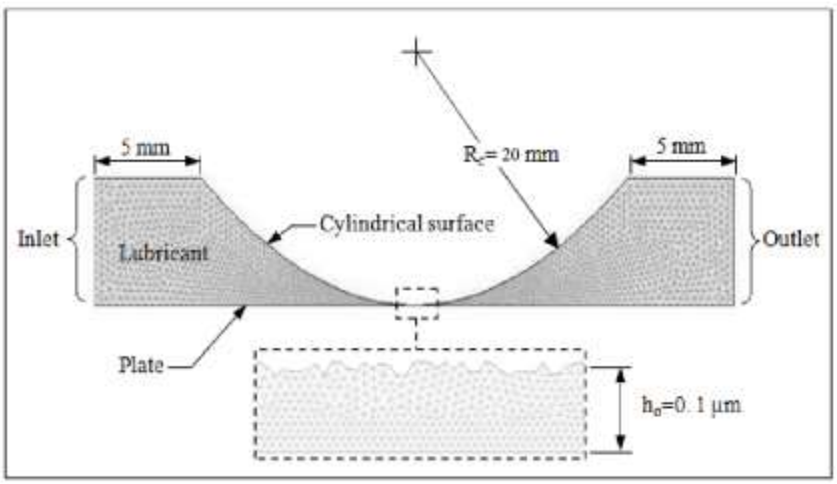

Fig. 1. The CFD model of the EHL problem with surface roughness.

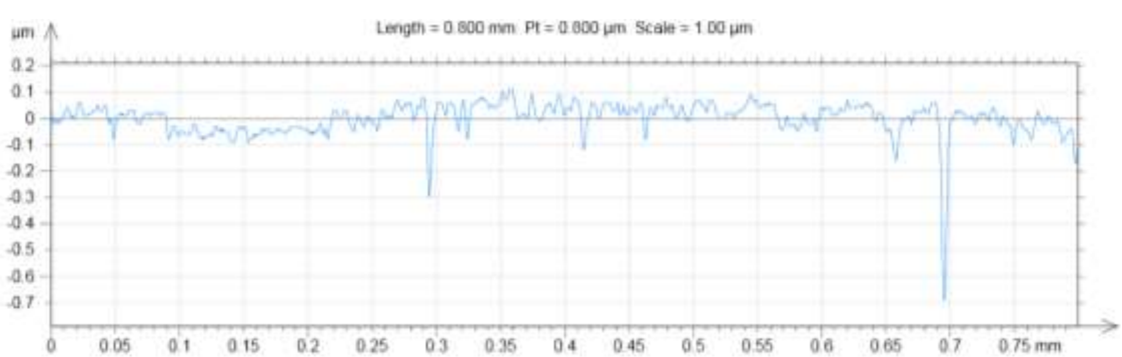

Fig. 2. A sample of the real rough profile on the cylindrical roller bearing.

2. 3. The Load Balance Equation

The moving direction of the cylinder that can be moved up or down is dependent on the balance of the generated pressure and the applied load. When the high load is applied on the cylindrical roller bearing it should be considered to be an elastic deformation. The proportion of the unbalanced force (*defect*) is used to calculate the displacement of the cylinder. The maximum displacement depends on the minimum mesh size (y_{min}), the generated pressure and the constant value c (which is chosen as 0.1 in this study). The undeformed gap can be evaluated from

$$h_o^{new} = h_o^{old} + \Delta y \tag{9}$$

where Δy is upon load and time step as following

$$\frac{d^2 y}{dt^2} \cong L - \int p dx \tag{10}$$

3. Results and Discussion

The grid independent tests have been conducted, and some optimized structured 11,484 quadrilateral cells are used in the models. The smallest face area and the largest face area used in the simulations are 3.41×10^{-8} m^2 and 8.68×10^{-4} m^2, respectively. The initial and boundary conditions need to be defined and the variables in the domain are calculated by using the velocity-pressure coupling method.

Table 1. Model parameters.

Parameters	Value	Unit
Input data		
- An applied load, W	79,920.88	N/m
- Average velocity, U_a	1	m/s
- Cylinder radius, R_c	20	mm
- Surface roughness, R_a	0.0275	µm
- Ambient temperature, T_0	313.0	K
Solid properties (cylinder and plate)		
- Elastic modulus of solids, E	200	GPa
- Poisson's ratio of solids, υ	0.3	-
- Specific heat of solids, C_p	460	J/Kg-K
- Density of solids, ρ	7850	kg/m^3
- Thermal conductivity, k	47	W/m-K
Lubricant properties		
- Inlet viscosity of lubricant, η_0	0.04	Pa·s
- Vapour dynamic viscosity, μ_v	$8.97\text{x}10^{-6}$	Pa·s
- Liquid density, ρ_l	846.0	kg/m^3
- Vapour density, ρ_v	0.0288	kg/m^3
- Inlet temperature of lubricant, T_0	313.0	K
- Thermal conductivity of lubricant, k	0.14	W/m-K
- Temperature-viscosity coefficient of lubricant, γ	0.00064	1/K
- Specific heat of lubricant, C_p	2,000	J/ Kg-K
- Thermal expansivity of lubricant, β	$4.5\text{x}10^{-4}$	1/K
- Pressure -viscosity index, z	0.4836	-

The transport equation in general discretized form can be solved iteratively for all elements in the domain. In order to obtain the pressure, velocity and temperature, the common parameters as shown in table 1 are used and then the velocity and pressure fields are approximated for the first iteration. These parameters are then used to solve the momentum equation, the pressure correction equation and energy equation. The new values of the pressure, velocity and temperature will be corrected in each iteration, until the acceptable convergence of pressure and velocity is smaller than 10^{-4}.

In this study, the CFD model result is compared with the result from the Reynolds equation as published in the paper by Chu et al. (2009) as defined in Figure 3. The lubricant in this case is assessed as a Newtonian fluid, and the thermal effect is taken into consideration in the calculation of viscosity and density. It can be seen that the pressure distribution and film thickness of the CFD model and the Reynolds equation are in good agreement. The maximum error of the peak pressure is 0.78%, and the maximum error of the minimum film thickness is 1.73%.

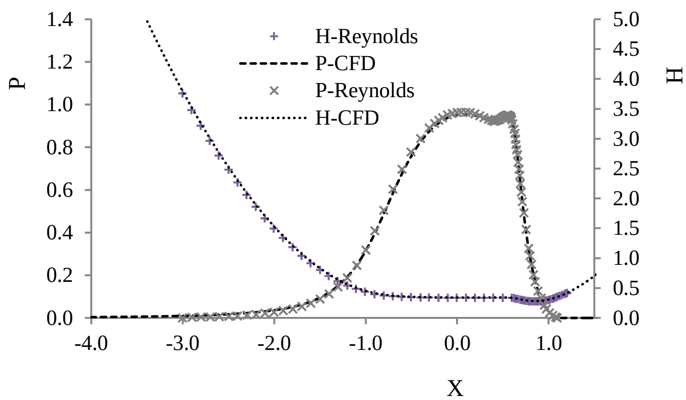

Fig. 3. Comparison of dimensionless pressure distribution and film thickness between the CFD model and the Reynolds equation.

Figure 4 shows the comparison of the pressure distribution between the smooth surface case and the rough surface case under pure rolling, rolling-sliding and pure sliding conditions. It can be clearly seen that the surface roughness influences significantly the pressure distribution, especially in the pure sliding case.

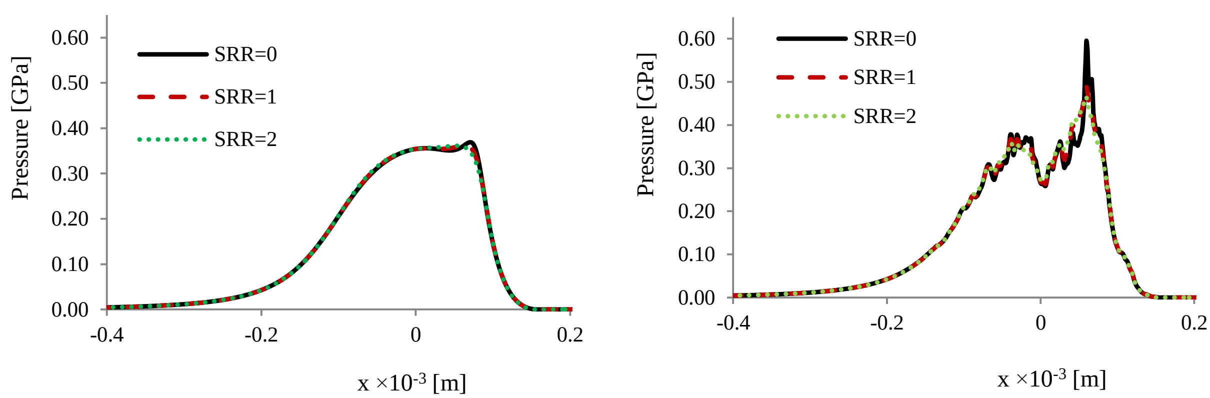

Fig. 4. Comparison of the pressure distribution between smooth surface (left) and rough surface (right) cases at SRR=0, 1 and 2

Figure 5 shows the contours of velocity at SRR=0, 1 and 2 for the TEHL problem with smooth surface and rough surface. The film thickness in the smooth case under the pure sliding condition is slightly thinner than those under the other two conditions as the temperature rise and pressure distribution of this case are higher than the other two conditions. Figure 5 shows the comparison of the pressure distribution between the smooth surface case and the rough surface case under pure rolling, rolling-sliding and pure sliding conditions. It can be clearly seen that the surface roughness influences significantly the pressure distribution, especially in the pure sliding case.

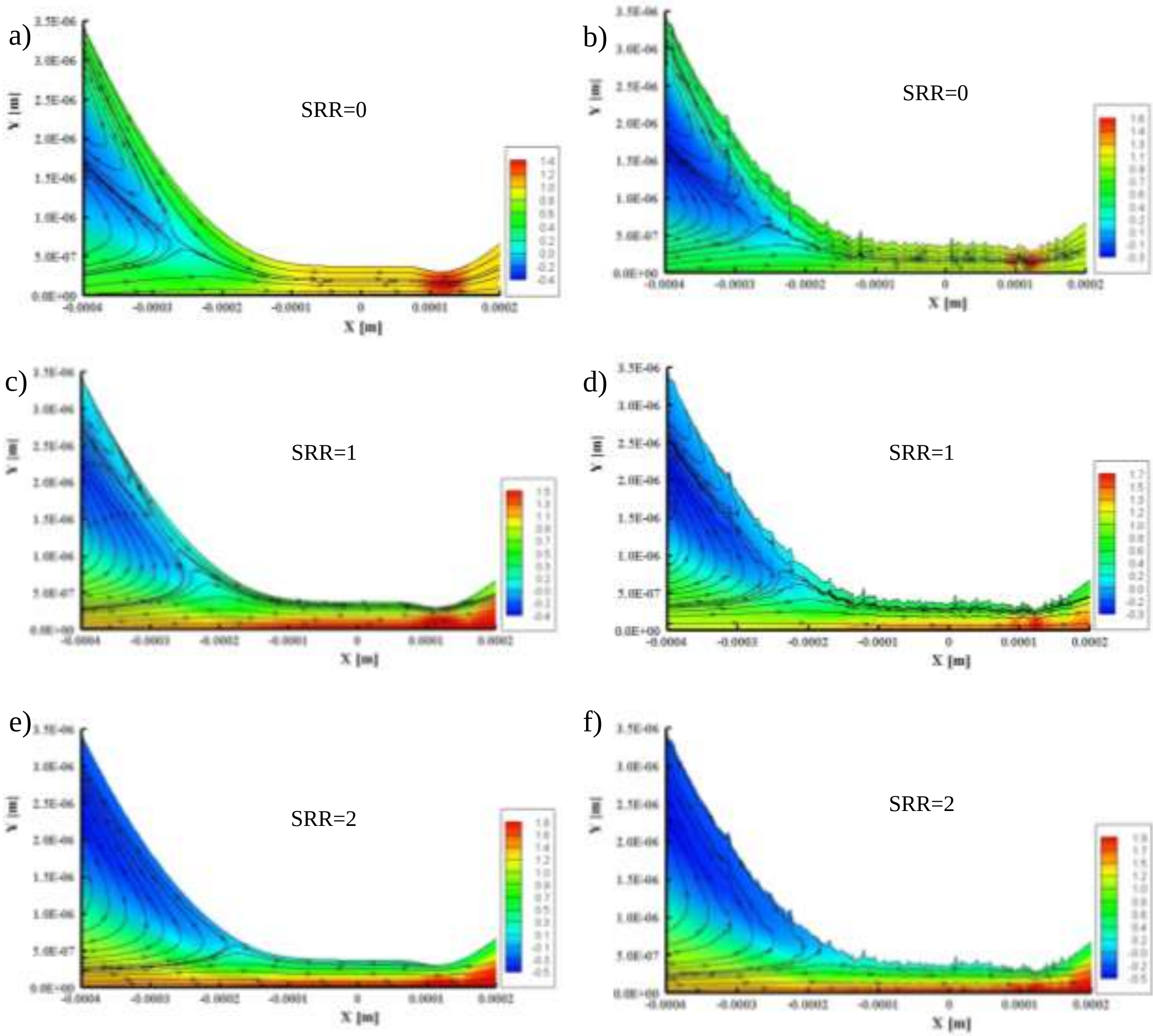

Fig. 5. Comparison of the velocity (m/s) between the smooth surface (left) and the rough surface (right) case at SRR=0, 1 and 2

It can also be clearly seen that the temperature rises significantly when the shear stress is increased, as shows in Figure 6. The temperature at the minimum film thickness point is the highest as the velocity in this area is the highest and both drop dramatically after flow passes through the outlet region. The temperature contours are also shown that the highest temperature is about 339.4 K in the case of pure sliding with rough surface, and the highest temperatures with rough surface are around 3 K, 6 K and 10 K, respectively, which are higher than the corresponding smooth surface cases.

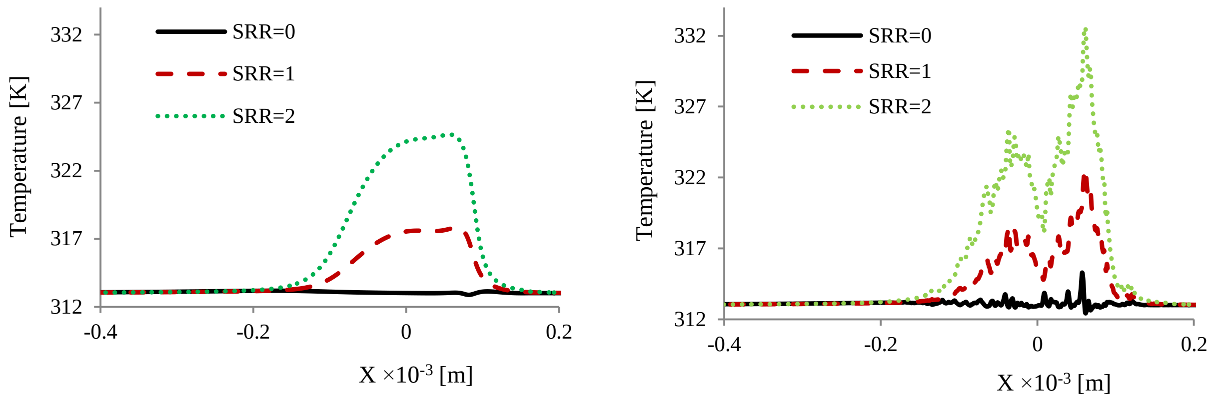

Fig. 6. Comparison of temperature distribution on the surface of cylinder between the case of smooth surface (left) and the rough surface (right) at SRR=0, 1 and 2.

4. Conclusion

The CFD model has been used successively to simulate the pressure distribution, the generated temperature, the viscosity and the velocity of lubricant under the varied slide to roll conditions. The results show that the CFD model can be a useful tool for the TEHL line contact problem, and can deal with the cavitation problem. In particular, it is found that

- The rough surface is the cause of the streamwise flow fluctuation.
- The temperature at the contact centre is highest at pure sliding condition and some of heat transfers from the fluid to solid.
- The pressure peak and the temperature rise at the contact centre for the rough surface case are higher than the corresponding smooth surface case.

Acknowledgements

The authors gratefully acknowledge the financial support on the project from the Ministry of Science and Technology of Thailand.

References

Ai, X., Cheng, S.H., (1994) A Transient EHL Analysis for Line Contacts with Measured Surface Roughness Using Multigrid Technique, *Tran. ASME. Journal of Tribology*, 116, pp. 549-558.

Almqvist, T., Larsson, R., (2002) The Navier-Stokes Approach for Thermal EHL Line Contact Solutions, *Tribology International*, 35(3), pp. 163-170.

Almqvist, T., Larsson R., (2008) Thermal Transient Rough EHL Line Contact Simulations by Aid of Computational Fluid Dynamics, *Tribology International*, 41(8), pp. 683-693.

Bruyere, V., Fillot, N., Morales-Espejel, G.E., Vergne, P., (2011) Computational Fluid Dynamics and Full Elasticity Model for Sliding Line Thermal Elastohydrodynamic Contacts, *Tribology International*. 46(1), pp. 3-13.

Chu L-M, Hsu H-C, Lin J-R, Chang Y-P., (2009) Inverse approach for calculating temperature in EHL of line contacts. TribologyInternational. 42:1154-62.

Dowson, D., (1962) A Generalized Reynolds Equation for Fluid-Film Lubrication, *International Journal of Mechanical Sciences*, 4(2), pp. 159-170.

Dowson, D., G.R. Higginson, (1959) A numerical solution to the elasto-hydrodynamic problem. Journal of Mechanical Engineering Science.1:6-15.

Dowson D, Higginson G.R., (1966) Elastohydrodynamic Lubrication, The Fundamentals of Roller and Gear Lubrication, Oxford :Pergamon Press.

Hamrock BJ, Dowson D., (1976) Isothermal elastohydrodynamic lubrication of point contacts. Part 1-theoretical formulation. Journal of tribology -Transactions of the ASME. 98:223-9.

Hartinger, M., Dumont, M.L., Ioannides, S., Gosman, D., Spikes, H., (2008) CFD Modeling of a Thermal and Shear-Thinning Elastohydrodynamic Line Contact, *Journal of Tribology*, 130(4), pp. 179-180.

Hertz H., (1881) Über die Berührung fester elastischer Körper. Journal für die reine und angewandte Mathematik. 92:156-71

Lee, R. T., Hsu, C.H., (1994) Advanced Multilevel Solution for Thermal Elastohydro- dynamic Lubrication of Simple Sliding Line Contacts, *Wear*, 171 , pp. 227-237.

Lubrecht, A.A., T.N. W.E., Bosma R., (1987) Multigrid, an Alternative Method of Solution for Two-Dimensional Elastohydrodynamically Lubricated Point Contact Calculations, *Trans. ASME. Journal of Tribology*, 109, pp. 437-443.

Okamura, H., (1983) A Contribution to the Numerical Analysis of Isothermal Elastohydro- dynamic Lubrication, *Proc. 9th Leeds-Lyon Symp. on Tribology*, pp. 313-320.

Osborn, K.F., Sadeghi, F., (1992) Time Dependent Line EHD Lubrication Using the Multigrid/Multilevel Technique, *ASME. Journal of Tribology*, 114, pp. 68-74.

Petrusevich, A.I., (1951) Fundamental conclusions from the contact-hydrodynamic theory of lubrication, *Izv. Akad. Nauk. SSSR (OTN)*, vol. 2, pp. 209-223.

Reynolds, O., (1886) On the Theory of Lubrication and Its Application to Mr. Beauchamp Tower's Experiments, Including an Experimental Determination of the Viscosity of Olive Oil, *Philosophical Transactions of the Royal Society of London*, 177, pp. 157-234.

Venner, C.H., Ten Napel, W.E., (1992) Surface Roughness Effects in an EHL Line Contact, *ASME Journal of Tribology*, 114, pp. 616-622.